Kinetics of the Reaction of SO_2 with Calcined Limestone

R. H. Borgwardt

National Air Pollution Control Administration
Public Health Service
Department of Health, Education, and Welfare
Cincinnati, Ohio 45227

Processes in which limestone and dolomite are used to desulfurize flue gas are being intensively investigated under the sponsorship of the National Air Pollution Control Administration. Such processes include dry injection of pulverized stone into boiler furnaces and the use of fluidized bed contactors, fluid bed combustion, and thin fixed-beds.

It is generally assumed that limestone absorbs SO_2 by a mechanism involving two consecutive steps, dissociation of the calcium carbonate followed by reaction of CaO with sulfur dioxide. It is expected that the rate of the second step will be important in any of the proposed pollution control processes, and especially in the dry injection process (Potter, 1968). Several investigators (Harrington, 1968, Potter, 1969) have determined the saturation capacities of a large number of naturally occurring limestones and dolomites under various conditions of reaction with SO_2. Other studies under way will define the rate of reaction of uncalcined limestones in the disperse phase (Lougher and Coutant, 1968). The purpose of the investigation reported in this paper is to determine the rate of reaction of limestones after calcination under standardized conditions.

Experimental

Complete geological descriptions of the stones used in this work are given in a separate report (Harvey, 1968). The chemical composition and primary physical characteristics of the calcined stones are given in Table I. Calcination was carried out in 180-gm batches in a Inconel kiln 12.5 cm. long and 8 cm. in diameter rotated at 1 rpm. It was heated to 980°C in a muffle furnace and then charged with 10/28-mesh stone. The kiln was maintained at 980°C and purged with air for 2 hours to remove CO_2 during calcination. Conversion to the oxide was complete under these conditions (CO_2 < 0.5%). The calcined stone was cooled, crushed, and screened into size ranges of 14/16, 28/35, 42/65, and 150/170 mesh (Tyler). The calcined samples were stored in air-tight containers until used.

The rate of reaction with SO_2 was determined in a differential reactor (Figure 1) constructed of Inconel alloy. In this type of reactor the thin layer of solid and high gas flow prevent gas-phase concentration gradients in the reacting solid. The gases enter the bottom of the reactor housing, are passed upward through an annular preheat section 73 cm. long and 5.25 cm. in diameter and then back downward through the inner, concentric reactor tube containing the limestone sample. The outer diameter of the reactor tube is 4.13 cm., and the inner diameter 3.42 cm. The sample is supported on a 30-mesh Inconel screen in a removable carrier. The carrier is sealed against a flange in the center of the reactor tube so that the entire gas flow passes through the solid during exposure.

In this investigation a sample consisted of 30 milligrams of calcined stone, which was distributed uniformly over the 2.65-cm. diameter screen. For small particle sizes a disk of woven refractory fabric was placed on the screen and a 1-cm. thickness of refractory (fused quartz) gauze on the fabric. The lime particles were dispersed into the gauze.

The mass flow rate of gas through the screen was matintained constant at 0.075 gm/(cm^2) (sec), which at 870°C corresponds to a superficial velocity of 240 cm/sec. A high gas velocity reduced gas film resistance to a negligible value so that mass transfer to the particle surface did not affect rate measurements. The gas fed to the reactor was a flue gas generated by combustion of fuel oil containing carbon disulfide. The composition of the flue gas was 10.5% CO_2, 3.4% O_2, 9.9% H_2O, 0.27% SO_2, 0.003% SO_3, and 75.9% N_2. The sulfur dioxide concentration was monitored continuously with a Beckman Mod. 315 infrared analyzer.

The reactor was mounted in an electric furnace containing three heating sections. The center section was energized by a proportional controller acting on a thermocouple located 3.4 cm. above the screen supporting the lime sample. The other two sections were equipped with variable transformers set by thermocouples in the top and bottom of the reactor tube to maintain a uniform temperature over the full length of the reactor and preheater assembly. The thermocouples were calibrated in situ against a multiply shielded, high-velocity thermocouple. A mulitpoint recorder continuously monitored reactor temperatures.

Before a run was started, the carrier and sample were allowed to heat up for 5 minutes to the reactor temperature. The time of exposure of the solid to the gas stream was controlled by solenoid valves that started the gas flow at the beginning of the run and purged the reactor with nitrogen at the end of the run. The sample was removed from the carrier after exposure (along with the refractory gauze, if used) and analyzed for sulfate. The exposed sample was dissolved by treatment with ion exchange resin, filtered, and titrated in 80% isopropyl alcohol with barium perchlorate using thorin indicator.

Results and Discussion

The chemical reaction between limestone and sulfur dioxide at high temperature in the presence of excess oxygen is:

$$CaO + SO_2 + 1/2\ O_2 \rightleftharpoons CaSO_4 \qquad (1)$$

Equilibrium data for the reaction have been summarized by researchers at Battelle Memorial Institute (1967). The reaction proceeds to the right at temperatures up to 1230°C at partial pressures of SO_2 corresponding to flue gas concentrations of about 3000 ppm. The MgO component of dolomite has been reported to participate in the reaction also in the presence of iron oxide impurities (Wickert, 1963). No distinction is made in this study between CaO and MgO, although the data suggest that CaO is the only significantly reactive component at the temperatures investigated. When reaction (1) takes place in flue gas containing high concentrations of carbon dioxide, equilibrium also favors a competing reaction (Battelle, 1967) below 770°C:

$$CaO + CO_2 \rightleftharpoons CaCO_3 \qquad (2)$$

Typical experimental results for the sorption of SO_2 are shown in Figure 2; the milligrams SO_3 found in 150/170-mesh particles (Dp = .0096 cm) after reaction is plotted against exposure time at various reaction temperatures. Figure 3 shows a similar plot for different particle sizes at a reaction temperature of 870°C. Total conversion of the CaO would correspond to an ordinate value of 23.2 mg. These figures illustrate the strong sensitivity of the reaction to temperature and the surprisingly low sensitivity to particle size, which were characteristic of all the stones examined.

The rate of sorption was measured as the tangent to the smooth curve drawn through the data and is defined as:

$$r = \frac{1}{W}\frac{dn'}{dt} \qquad (3)$$

where W is the grams calcined stone exposed in the reactor and n' is the gram moles of SO_3 in the stone at time t.

The data were correlated according to the rate expression for chemical reaction in a porous solid (Satterfield & Sherwood, 1963):

$$-\frac{dn}{dt} = k_v V C^m \eta \qquad (4)$$

since $dn'/dt = -dn/dt$

$$\frac{1}{W}\frac{dn'}{dt} = \frac{\eta}{\rho} k_v C^m \qquad (5)$$

The effect of SO_2 concentration, C, on the reaction rate is shown in Figure 4 for dolomite 1337. The SO_2 concentration was varied between 58 and 6000 ppm by changing the carbon disulfide content of the fuel oil burned in the furnace. The reaction rate was measured at a conversion of 10.5% of the CaO in 14/16-mesh stone reacted at 870°C. The line fitted to these data by the method of least mean squares has a slope of 1.088 or $m \approx 1$, indicating that the reaction is first order with respect to the concentration of SO_2 in the gas phase. The SO_2 concentration was fixed at a value of 2.88×10^{-8} gm mole/cm^3 (3000 ppm, dry) for the remainder of the experimental work, which is reported below.

The rate constant k_v is a function of temperature and also some function of n'/W, the sulfate loading; it decreases as the reaction progresses and the solid reactant is consumed. The temperature dependency of the sorption rate was correlated by the Arrhenius equation:

$$k_v = Ae^{-E/RT} \qquad (6)$$

An Arrhenius plot for each of the four calcined stones is shown in Figure 5 for reactions at temperatures between 650 and 980°C. The rates were measured at a sulfate loading of 0.9×10^{-3} gm mole/gm of 150/170-mesh particle size sample. The data show a linear correlation between log r and 1/T, as specified by equations (5) and (6). The apparent activation energy determined from the slope of these plots was distinctly different from each stone, ranging from 8.1 to 18.1 K cal/gm mole. When rates were measured at higher CaO conversions - up to 20% - the plots shifted toward the abscissa, but remained parallel to the lines shown in Figure 5, thus indicating no significant change in the activation energy.

The high sensitivity of the rate of sorption to temperature suggests chemical reaction to be the predominant rate-controlling resistance. The apparent activation energy for sorption controlled solely by bulk diffusion would be only 3.4 K cal/gm mole. A summary of the empirical kinetic parameters estimated from these data are given in Table II.

The plots further indicate that reduction in rate of reaction with SO_2 as a result of completion with CO_2, was not important at 650°C. At 540°C, however, there was evidence that reaction (2) was significant and the Arrhenius plots could not be extrapolated to that temperature. The plots also failed when the reaction temperature was raised from 980 to 1100°C, sorption rates decreasing at the higher temperature. Subsequent experiments in which the calcine was heated for 10 minutes at 980°C and then reacted at 870°C showed the same difference in rate when compared to a sample which was not exposed to the high temperature. It was

concluded that the loss of reactivity was due to the changes in porosity and bulk density which occur when lime is "overburned" (Boynton, 1966).

The effect of particle size on reaction rate is shown in Figure 6 in which the value of r at a sulfate loading of 1.8×10^{-3} gm mole/gm is plotted against the inverse of particle diameter. If the particles are assumed to be spherical, the total exterior surface of a given mass of stone (specific surface) would increase with $1/D_p$ when the particle size is reduced. Also, if the reaction occurs only at the outer surface, the plot shown in Figure 6 would be expected to be a straight line through the origin. It is clear that the rate was not proportional to specific surface and in some cases was essentially independent of it. The results suggest that some reaction takes place within the interior structure of the solid and that the relative importance of the internal reaction becomes greater as the particle size decreases. These observations are similar to the effects associated with highly porous catalysts and are consistent with the fact that the pore space in calcined limestones usually accounts for 50% or more of the total volume of the particles. The porosities (or fraction of particle volume that is pore space) for the 4 calcined stones are given in Table 2.

Figure 7 shows the conversion vs. time response for different particle sizes of stones 1351 and 1343 over long periods of exposure at 870°C. An analysis of the response according to the method of Shen and Smith (1965) was made to test for intra-particle shell diffusion. This model is based on diffusion through the product crust as the rate limiting mechanism and a non-porous solid reactant in which reaction occurs only at the interface of the unreacted core. The data from this investigation could not be correlated by the shell diffusion model when different particle sizes were considered. Figure 6 shows that the shell diffusion model, which predicts that the rate of sorption at a given sulfate loading will increase with $1/D_p^2$ is clearly inconsistent with data on particle size vs. reaction rate. This anomaly can only be explained if the effective diffusion coefficient decreases with particle size. Stone 1343, for example, had a diffusion coefficient of 3.4×10^{-2} cm^2/sec for 14/16-mesh particle size, but only 0.054×10^{-2} cm^2/sec for 150/170-mesh particle size.

The data could be correlated empirically over the full course of reaction by a plot of log r against sulfate loading, n'/W, as shown in Figure 8. The data could be linearized in this manner for all particle sizes of each of the four stones examined at a reaction temperature of 870°C. The observed response can be interpreted in terms of a change in the frequency factor, A, of equation (5). The frequency factor, which relates the reaction rate to the number of molecular collisions occurring per unit volume per unit time, is dependent upon the amount of SO_2 and the amount of CaO present. As the reaction progresses and CaO is consumed, the frequency factor decreases in some manner related to the amount of sulfate formed. Figure 8 suggests a relationship of the type:

$$A = A_o e^{-\beta n'/W} \qquad (7)$$

where A_o is the frequency factor at zero conversion and β is an emperical factor dependent upon particle size.

The correlation of Figure 8 has several implications regarding reaction kinetics. First, it shows that the rate is more sensitive to sulfate loading for large particles than it is for small particles. Second, it shows that the initial rate at zero loading may be estimated so that the effectiveness factor may be evaluated. The data shown for stone 1337 indicate that the effectiveness factor was not unity in this case. Other stones showed less change in η with particle size.

The results of this study show that the rate of sorption of SO_2 by calcined limestones is dependent to a very large extent upon the kinetics of the chemical reaction, particularly at small particle sizes and that the rate of reaction predominates as the overall rate-controlling resistance for conversion of at least the first 20% of the CaO.

Acknowledgement

The author thanks Mr. Robert Larkin for development of the procedure for analysis of sulfate in limestone.

Nomenclature

A	frequency factor, sec^{-1}
A_o	frequency factor at zero solid conversion, sec^{-1}
C	gas phase concentration of sulfur dioxide, gm moles/cm^3
$\overline{D}_p$	mean particle diameter, cm
E	activation energy, cal/gm mole
k_v	reaction rate constant per unit volume of solid, sec^{-1}
m	order of reaction with respect to sulfur dioxide
n'	sulfate in solid as SO_3, gm moles
R	gas constant, 1.987 (cal/gm mole °K)
r	reaction rate with respect to formation of SO_3 in the solid, gm mole/(sec)(gm)
V	total volume of solid, cm^3
W	weight of solid sample, gm
T	temperature, °K
t	time, sec
β	empirical correlation factor defined by equation (7)
η	effectiveness factor, ratio of reaction rate to the rate that would obtain if entire volume of particle participated equally in reaction
ρ	bulk density of solid, gm/cm^3

Literature Cited

Boynton, R. S., "Chemistry and Technology of Lime and Limestones", John Wiley and Sons, New York (1966).

Coutant, et. al., "Investigation of the Reactivity of Limestone and Dolomite for Capturing SO_2 from Flue Gas", Interim report submitted by Battelle Memorial Institute for contract No. PH 86-67-115 (August 30, 1968).

Harrington, R. E., Borgwardt, R. H. and Potter, A. E., American Industrial Hygiene Assoc. J., 29, 152-8 (1968).

Harvey, R. D., Environmental Geology Notes, 21, (1968).

Satterfeld, C. N., and Sherwood, T. K., "The Role of Diffusion in Catalysis", Addison-Wesley, Reading, Mass. (1963).

Shen, J. and Smith, J. M., Industrial & Eng. Chem. Fund., 4 (3), 293-301 (1965).

Potter, A. E., Harrington, R. E., and Spaite, P. W., Air Engineering, 22-6 (April, 1968).

Potter, A. E., "Sulfur Oxide Capacity of Limestones", manuscript in review for publication.

Ward, J.J., et. al., "Fundamental Study of the Fixation of Lime and Magnesia". Report submitted by Battelle Memorial Institute on completion of PHS Contract No. PH 86-66-108 (June 30, 1966).

Wickert, K., Mitteilungen der VGB, 83 74-82 (1963).

Table I. Properties of Calcines

Sample	LoI[a]	% CaO	%MgO	% Fe_2O_3	% SiO_2	Bulk (particle) Density,[b] ρ gm/cm^3	Porosity[b] cm^3/cm^3
1337	47.4	55	43	0.33	0.92	1.41	0.60
1351	42.4	54	28.5	7.0	8.2	1.59	0.56
1343	42.8	94	0.8	0.66	2.98	1.88	0.45
1360	43.8	81	13.0	1.25	3.65	1.51	0.56

(a) weight loss on calcination

(b) 150/170 mesh particle size

Table II. Kinetic Parameters[a] for Sorption of SO_2 by Calcined Limestones

Stone	Activation Energy, E Cal./gm mole	Reaction Rate Constant, K_v sec^{-1}	Frequency Factor, A sec^{-1}
1337	10,000	4.8×10^3	2.4×10^5
1351	18,100	7.2×10^3	9.0×10^6
1343	14,200	4.0×10^3	1.1×10^6
1360	8,100	2.3×10^3	5.5×10^4

(a) evaluated at sulfate loading of 0.9×10^{-3} gm mole/gm, 150/170 mesh particle size.

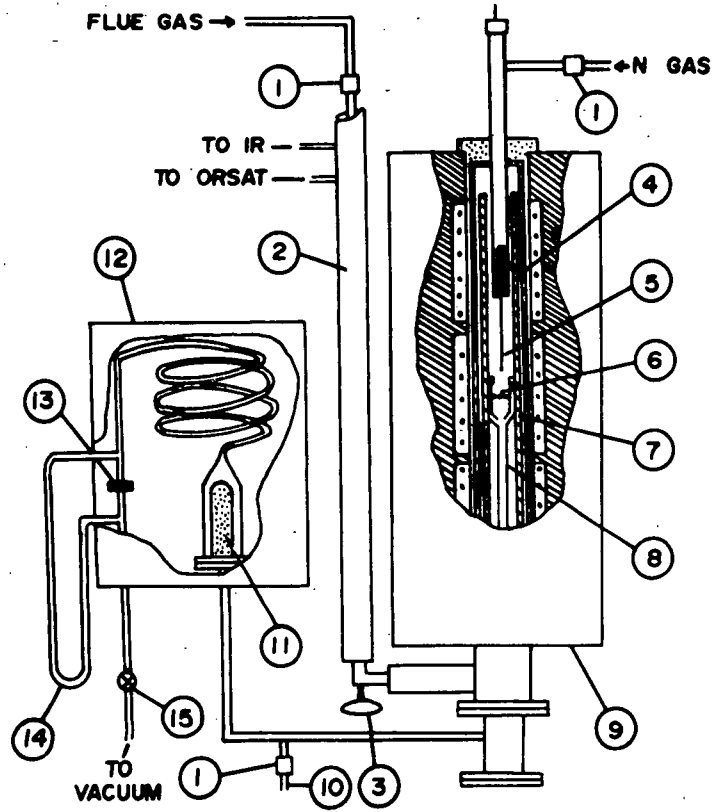

Figure 1. Apparatus

1. Teflon Solenoid valve 2. Heating tapes 3. Thermometer 4. Preheat section 5. Thermocouple 6. Sample 7. Reactor tube 8. Carrier 9. Heating Furnace 10. N_2 Purge exhaust 11. Alundum filter 12. Constant temperature oven 13. Orifice 14. Manometer 15. Flow control valve

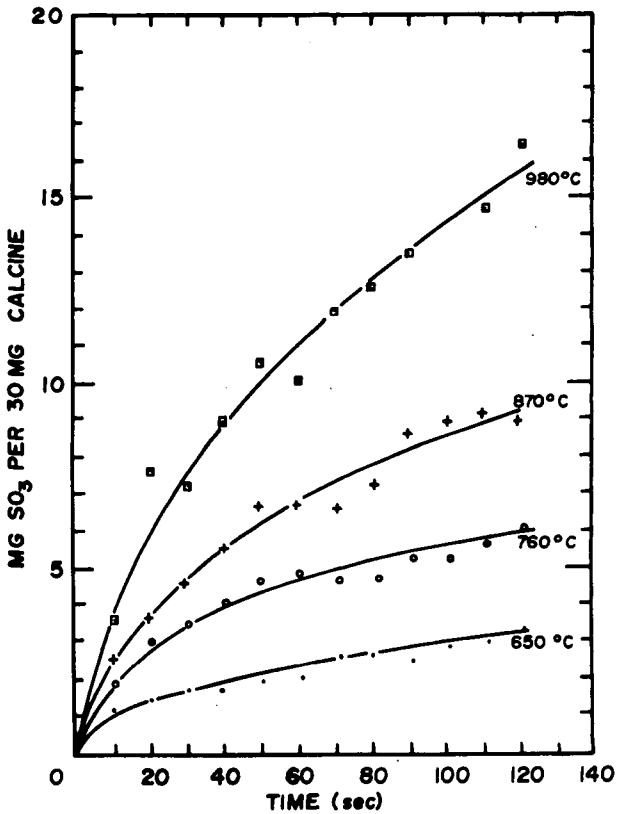

Figure 2. Sorption of sulfur dioxide by dolomite 1351 at various reactor temperatures

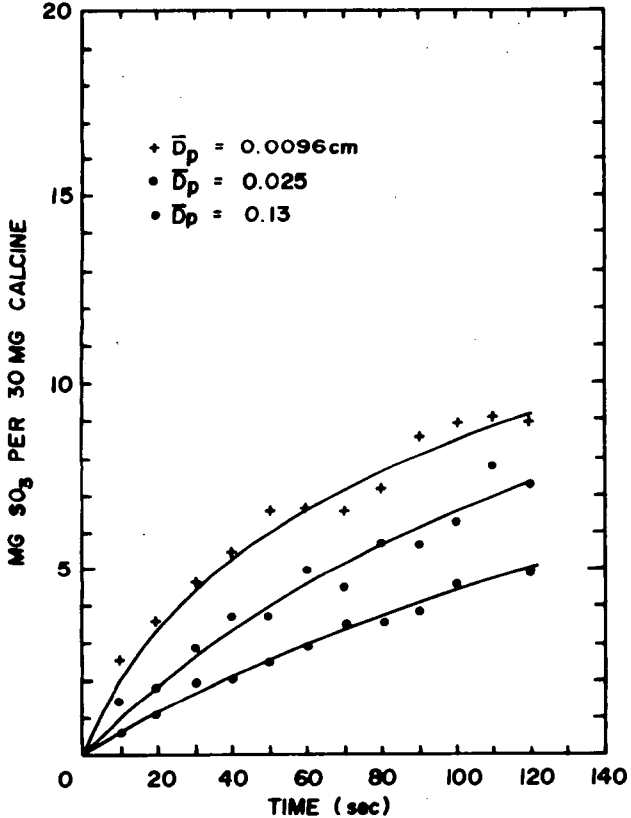

Figure 3. Sorption of sulfur dioxide by different particle sizes of dolomite 1351.

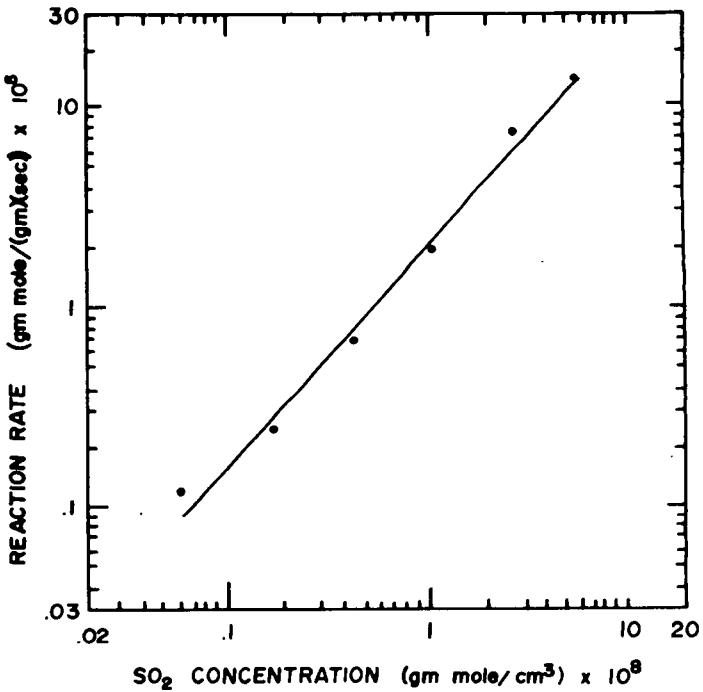

Figure 4 Log r vs. Log C to estimate m

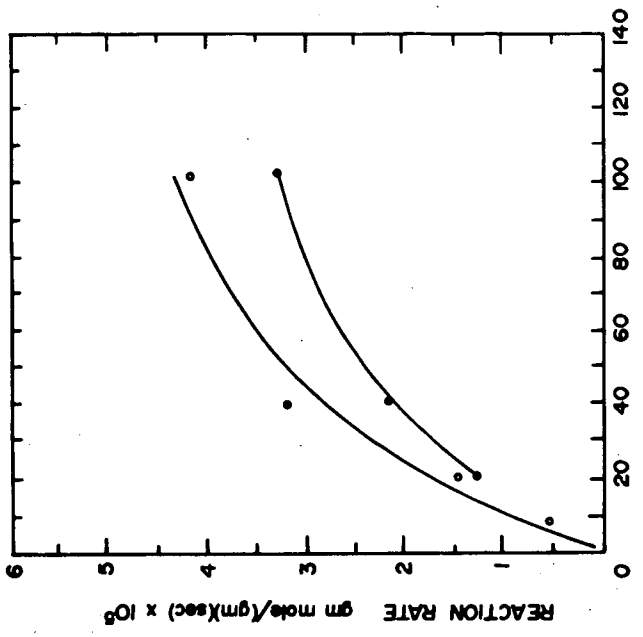

Figure 6. Reaction rate vs. $1/D_p$

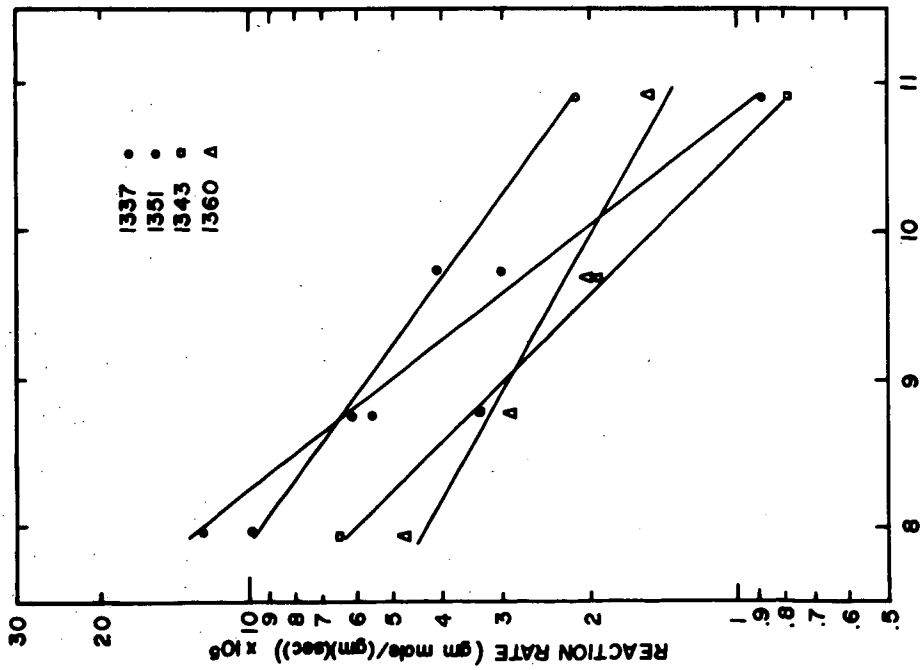

Figure 5. Arrhenius plots for the sorption of sulfur dioxide by four limestones

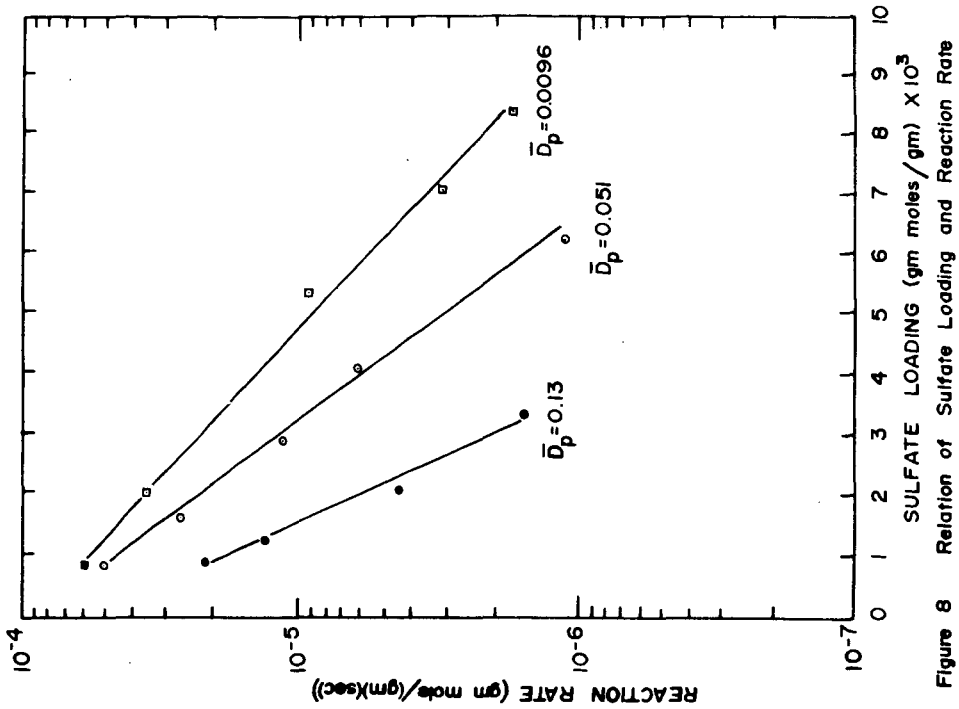

Figure 8 Relation of Sulfate Loading and Reaction Rate

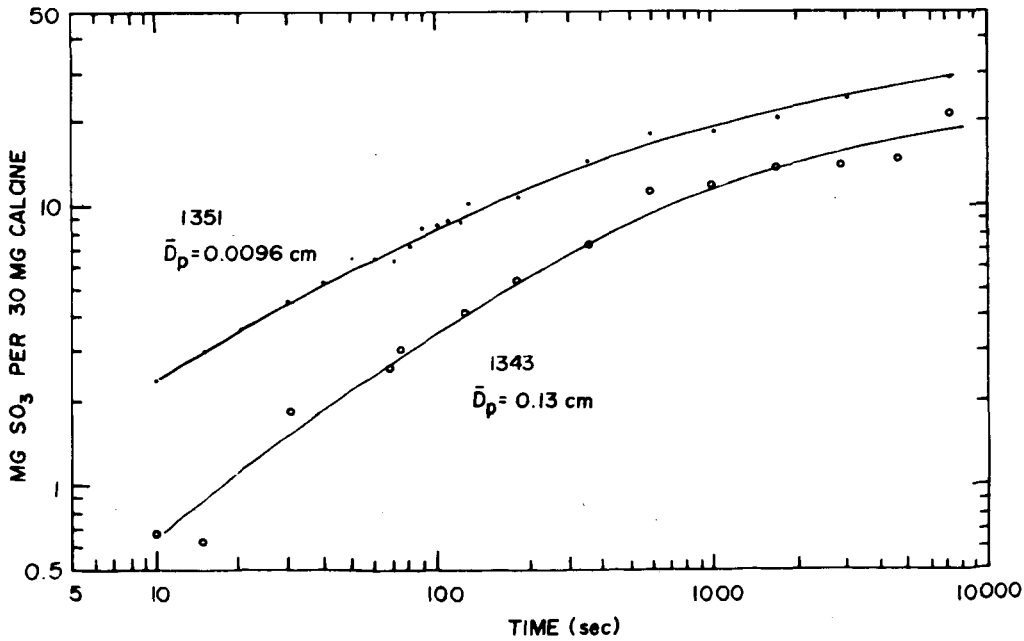

Figure 7 Sorption of sulfur dioxide by calcined limestone